

Cite this: *Dalton Trans.*, 2019, **48**, 16993

# Dioxygen reactivity of iron(II)–gentsiate/1,4-dihydroxy-2-naphthoate complexes of N4 ligands: oxidative coupling of 1,4-dihydroxy-2-naphthoate†

Rubina Rahaman,‡§ Sandip Munshi,§ Sridhar Banerjee, Biswarup Chakraborty, Sarmistha Bhunia<sup>†</sup> and Tapan Kanti Paine<sup>†\*</sup>

The influence of supporting ligands and co-ligands on the dioxygen reactivity of a series of iron(II) complexes, [(6-Me<sub>3</sub>-TPA)Fe<sup>II</sup>(GN-H)]<sup>+</sup> (**1**), [(6-Me<sub>3</sub>-TPA)Fe<sup>II</sup>(DHN-H)]<sup>+</sup> (**1a**), [(BPMEN)Fe<sup>II</sup>(GN-H)]<sup>+</sup> (**2**), [(BPMEN)Fe<sup>II</sup>(DHN-H)]<sup>+</sup> (**2a**), [(TBimA)Fe<sup>II</sup>(GN-H)]<sup>+</sup> (**3**), and [(TBimA)Fe<sup>II</sup>(DHN-H)]<sup>+</sup> (**3a**) (GN-H<sub>2</sub> = 2,5-dihydroxybenzoic acid and DHN-H<sub>2</sub> = 1,4-dihydroxy-2-naphthoic acid) of N4 ligands, is presented. The iron(II)–gentsiate complexes react with dioxygen to afford the corresponding iron(III) species. On the contrary, DHN-H undergoes oxidative C–C coupling to form [2,2′-binaphthalene]-1,1′,4,4′-tetrone 3-hydroxy-3′-carboxylic acid (BNTHC) on **1a**, and [2,2′-binaphthalene]-1,1′,4,4′-tetrone 3,3′-dicarboxylic acid (BNTD) on **2a** and **3a**. In each case, the reaction proceeds through an iron(III)–DHN species. The X-ray single crystal structures of [(6-Me<sub>3</sub>-TPA)Fe<sup>III</sup>(BNTD)] (**1<sup>Ox</sup>**) and [(BPMEN)Fe<sup>III</sup>(BNTD)] (**2<sup>Ox</sup>**) confirm the coupling of two DHN-H molecules. The formation of iron(III) product without any coupling of co-ligand from the complexes, [(BPMEN)Fe<sup>II</sup>(HNA)]<sup>+</sup> (**2b**) and [(BPMEN)Fe<sup>II</sup>(5-OMeSA)]<sup>+</sup> (**2c**) (HNA = 1-hydroxy-2-naphthoate, 5-OMeSA = 5-methoxysalicylate) confirms the importance of *para*-hydroxy group for the coupling reaction. The unusual coupling of DHN-H by the iron(II) complexes of the neutral N4 ligands is distinctly different from the oxygenolytic aromatic C–C cleavage of DHN by the iron(II) complex of a facial N3 ligand.

Received 28th August 2019,  
Accepted 26th October 2019

DOI: 10.1039/c9dt03493e

rsc.li/dalton

## Introduction

Gentic acid (2,5-dihydroxybenzoic acid) serves as an intermediate in the bacterial biodegradation of aromatic and heteroaromatic compounds.<sup>1–4</sup> The nonheme iron enzyme, gentsiate-1,2-dioxygenase (GDO), catalyses the O<sub>2</sub>-dependent cleavage of the C1–C2 bond of aromatic ring of gentsiate to form maleylpyruvate (Scheme 1).<sup>5–10</sup> Cells acquire carbon and energy through the conversion of maleylpyruvate to central metabolites such as fumarate and pyruvate.<sup>11,12</sup> GDO belongs to the cupin superfamily of proteins having a conserved six stranded β-barrel fold.<sup>1</sup> Other related enzymes in this superfamily, 1-hydroxy-2-naphthoate 1,2-dioxygenase (HNDO) and

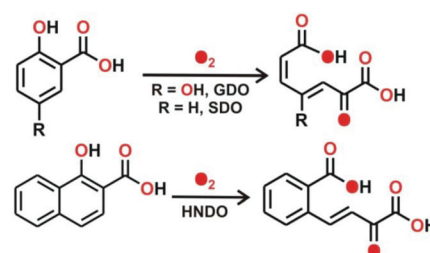
salicylate 1,2-dioxygenase (SDO), cleave the aromatic ring of 1-hydroxy-2-naphthoate and salicylate, respectively, to form the corresponding aliphatic compounds (Scheme 1). The aromatic C–C bonds of salicylate, gentsiate, 1-hydroxy-2-naphthoate and various monohydroxylated substrates are cleaved by SDO with high catalytic efficiencies.<sup>13,14</sup> In contrast, HNDO does not oxidize gentsiate or salicylate.<sup>15</sup> Similarly, GDO only catalyzes the oxidative cleavage of gentsiate, although it displays sequence similarity to HNDO and SDO. While salicylate and 1-hydroxy-2-naphthoate are not active substrates of GDO,<sup>3,5,7</sup> the relative activity of GDO is high against 1,4-dihydroxy-2-

School of Chemical Sciences, Indian Association for the Cultivation of Science, 2A&2B Raja S. C. Mullick Road, Jadavpur, Kolkata-700032, India.  
E-mail: ictkp@iacs.res.in

† Electronic supplementary information (ESI) available: Crystallographic data in CIF format and spectral data of the compounds. CCDC 1832200, 1832201, 1940079, 1832208 and 1832238. For ESI and crystallographic data in CIF or other electronic format see DOI: 10.1039/c9dt03493e

‡ Present Address: Department of Chemistry, Krishnagar Government College, Krishnagar, West Bengal-741101, India.

§ These authors contributed equally.



Scheme 1 Reactions catalysed by GDO and related enzymes.

naphthoate suggesting high specificity of GDO to dihydroxylated substrates.<sup>16</sup>

The crystal structure of GDO from *Escherichia coli* shows significant similarity to other proteins in the bicupin family and is a homotetramer containing one ferrous ion per tetramer.<sup>17</sup> Furthermore, the X-ray structure of GDO from *Silicibacter Pomeroyi* demonstrated that each mononuclear iron was coordinated by three histidines and three labile water molecules.<sup>15</sup> The binding of gentisate to the iron centre by replacing the labile water molecules initiates the oxygenative C–C bond cleavage reaction. While structural and biochemical studies on GDO provided mechanistic insights into the enzymatic reaction, bioinspired model chemistry using synthetic systems is less explored. We reported a five-coordinate iron(II) complex of a facial N3 ligand,  $[(\text{Tp}^{\text{Ph}_2})\text{Fe}^{\text{II}}(\text{DHN-H})]$  ( $\text{Tp}^{\text{Ph}_2}$  = hydrotris(3,5-diphenylpyrazolyl)borate and DHN-H = 1,4-dihydroxy-2-naphthoate) as the first functional model complex of GDO.<sup>18</sup> The model complex reacted with dioxygen to cleave the aromatic ring of DHN-H affording 2'-carboxy-4-hydroxybenzalpyruvic acid. Labelling experiments with  $^{18}\text{O}_2$  suggested the incorporation of two labeled oxygen atoms into the cleavage product exhibiting typical dioxygenase-type reactivity.<sup>18</sup> The non-innocent nature of the DHN allowed the reaction with dioxygen on the  $(\text{Tp}^{\text{Ph}_2})\text{Fe}^{\text{III}}$  unit resulting in aromatic C–C bond fission following intradiol cleavage pathway. Unlike the enzymatic system, the model complex was initially oxidized to an iron(III)–DHN complex, which further reacted with dioxygen to display C–C cleavage reaction. It has also been shown that the cleavage reaction took place only with aromatic carboxylates containing two *para* hydroxy groups.

The reaction pathway of iron(II)–gentisate complexes with dioxygen is expected to depend not only on the nature of substitution on gentisate but also on supporting ligand. To gain further insight into reaction pathways and to investigate the effect of ligands on the reactivity of model complexes, we have investigated several iron(II)–gentisate complexes of different supporting ligands of varying geometry (Chart 1). In this article, we report the synthesis, characterisation and dioxygen reactivity of a series of iron(II)–gentisate/1,4-dihydroxy-2-naphthoate complexes  $[(6\text{-Me}_3\text{-TPA})\text{Fe}^{\text{II}}(\text{GN-H})]^+$  (**1**),  $[(6\text{-Me}_3\text{-$

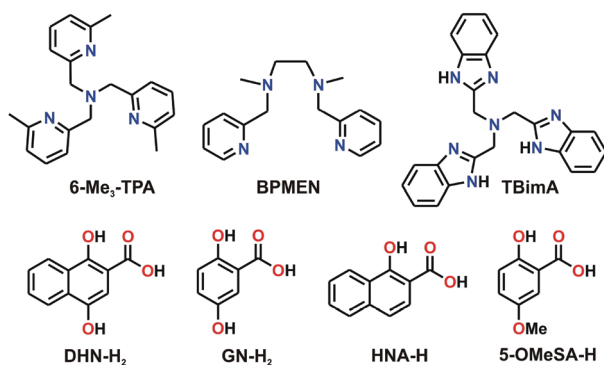


Chart 1 Supporting ligands and co-ligands used to prepare the ternary iron complexes.

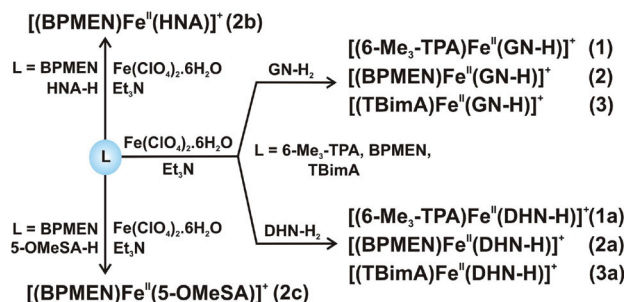
$\text{TPA})\text{Fe}^{\text{II}}(\text{DHN-H})]^+$  (**1a**),  $[(\text{BPMEN})\text{Fe}^{\text{II}}(\text{GN-H})]^+$  (**2**),  $[(\text{BPMEN})\text{Fe}^{\text{II}}(\text{DHN-H})]^+$  (**2a**),  $[(\text{TBimA})\text{Fe}^{\text{II}}(\text{GN-H})]^+$  (**3**), and  $[(\text{TBimA})\text{Fe}^{\text{II}}(\text{DHN-H})]^+$  (**3a**) (6-Me<sub>3</sub>-TPA = tris(6-methyl-2-pyridylmethyl)amine, BPMEN = (*N*<sup>1</sup>,*N*<sup>2</sup>-dimethyl-*N*<sup>1</sup>,*N*<sup>2</sup>-bis(2-pyridylmethyl)ethane-1,2-diamine, TBimA = tris(2-benzimidazolylmethyl)amine, GN-H<sub>2</sub> = 2,5-dihydroxybenzoic acid, DHN-H<sub>2</sub> = 1,4-dihydroxy-2-naphthoic acid) of different N4 ligands. In the reaction with dioxygen, the iron(II)–DHN-H complexes display an unusual C–C coupling of the co-ligand, whereas no such coupling is observed with the iron(II)–GN-H complexes. The reactivity of two related complexes,  $[(\text{BPMEN})\text{Fe}^{\text{II}}(\text{HNA})]^+$  (**2b**) and  $[(\text{BPMEN})\text{Fe}^{\text{II}}(5\text{-OMeSA})]^+$  (**2c**) (HNA = 1-hydroxy-2-naphthoate, 5-OMeSA = 5-methoxysalicylate), are presented for comparison.

## Results and discussion

### Synthesis and characterization

The iron(II) complexes were isolated from the reactions of the respective supporting ligand, iron(II) perchlorate with a basic solution of gentisic acid or 1,4-dihydroxy-2-naphthoic acid in methanol (Scheme 2). The complexes were characterized by different analytical and spectroscopic techniques such as IR, UV-vis, <sup>1</sup>H NMR, ESI-MS, and elemental analysis (Experimental section). The <sup>1</sup>H NMR spectra display well-resolved and paramagnetically shifted resonances typical of high-spin iron(II) complexes (Fig. S1–S8, ESI†). The analytical and spectral data support the composition of the complexes both in the solid state and in solution.

The binding mode of gentisate or 1,4-dihydroxy-2-naphthoate with the metal centre was established from the single crystal X-ray structures of **1** and **3a** (Table S1, ESI†). The solid-state structure of **1** reveals that the metal ion in the complex cation is coordinated by four nitrogen donors from the ligand and two carboxylate oxygen atoms of gentisate forming a distorted octahedral coordination geometry (Fig. 1a). The Fe–N distances range between 2.268(5) Å and 2.170(5) Å (Table 1). The Fe–O distances of 2.033(4) Å and 2.373(5) Å, respectively, suggest an asymmetric κ<sup>2</sup> coordination mode of the carboxylate group of gentisate. Similar asymmetric binding mode of carboxylate group has been reported in an iron(II)–benzoate complex of the ligand.<sup>19</sup> The phenolic OH group at *ortho* position of gentisate is in intramolecular hydrogen bonding interaction



Scheme 2 Synthesis of the iron(II) complexes.

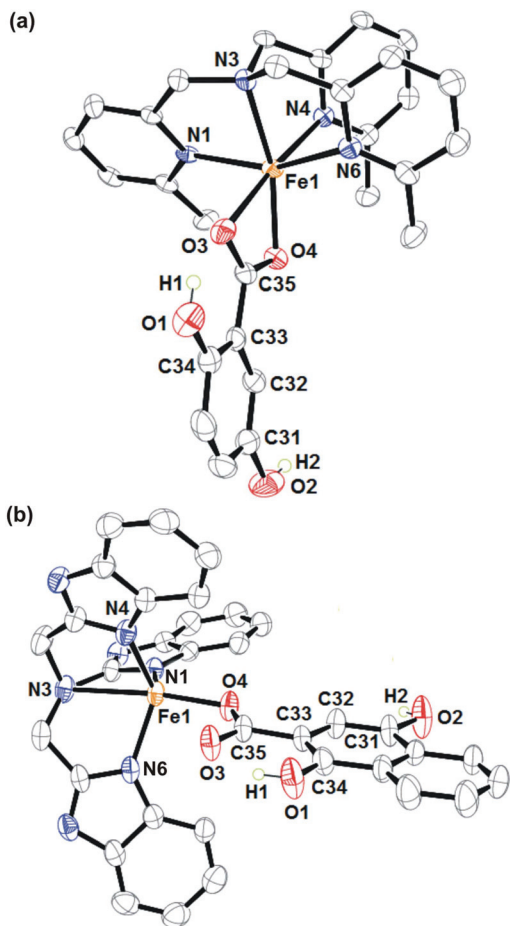


Fig. 1 ORTEP view of the cationic complex (a) **1** and (b) **3a** with 45% ellipsoid probability. Counter anion, solvent molecules, and the hydrogen atoms except those on O1 and O2 are omitted for clarity.

with the metal bound carboxylate oxygen O3 at a distance of 2.612 Å. The ligand wraps around the metal centre in such a geometry that the axial positions of the distorted octahedron are occupied by the carboxylate oxygen O4 and the pyridyl nitrogen N4 with the O3–Fe1–N4 angle of 173.0(2)° (Table 1).

The iron(II) complex **3a** was crystallized from a solvent mixture of dichloromethane and methanol at room temperature. In the monocationic complex, the iron centre is ligated by the N<sub>4</sub> donor TBimA ligand and a monoanionic 1,4-dihydroxy-2-naphthoate moiety (DHN-H) (Fig. 1b). The DHN-H coordinates in a monodentate mode through one carboxylate oxygen (O4) giving rise to trigonal bipyramidal coordination geometry ( $\tau = 0.72$ )<sup>20</sup> at the iron centre. The hydroxy groups of DHN-H remains non-coordinated similar to that reported for the iron(II)–DHN-H complex of the facial Tp<sup>Ph2</sup> ligand.<sup>18</sup> The iron–nitrogen bond distances match well with the reported high-spin iron(II) complexes of polydentate nitrogen ligands.<sup>21</sup> The iron–N<sub>amine</sub> bond is elongated to 2.476(9) Å similar to that observed in the reported iron(II) complexes of the TBimA ligand.<sup>21,22</sup> The amine nitrogen (N3) and the carboxylate oxygen (O4) occupy the axial positions with the N3–Fe1–O4

Table 1 Selected bond lengths (Å) and angles (°) for **1**·CH<sub>2</sub>Cl<sub>2</sub>·C<sub>2</sub>H<sub>10</sub>O and **3a**

	<b>1</b> ·CH <sub>2</sub> Cl <sub>2</sub> ·C <sub>2</sub> H <sub>10</sub> O	<b>3a</b>
Fe(1)–O(4)	2.033(4)	2.022(3)
Fe(1)–O(3)	2.373(5)	—
Fe(1)–N(1)	2.268(5)	2.093(3)
Fe(1)–N(3)	2.177(5)	2.476(9)
Fe(1)–N(4)	2.171(5)	2.102(4)
Fe(1)–N(6)	2.193(5)	2.122(3)
C(35)–O(4)	1.288(8)	1.288(4)
C(35)–O(3)	1.283(8)	1.271(4)
C(35)–C(33)	1.472(9)	1.513(4)
C(34)–C(33)	1.387(10)	1.390(4)
C(33)–C(32)	1.420(10)	1.425(5)
C(32)–C(31)	1.367(10)	1.374(4)
C(34)–O(1)	1.367(9)	1.355(4)
C(31)–O(2)	1.403(9)	1.395(4)
O(4)–Fe(1)–N(4)	119.17(19)	106.16(15)
O(4)–Fe(1)–N(3)	158.70(19)	172.3(3)
N(4)–Fe(1)–N(3)	82.14(19)	75.7(3)
O(4)–Fe(1)–N(6)	98.70(18)	99.90(14)
N(4)–Fe(1)–N(6)	98.15(19)	129.10(11)
N(3)–Fe(1)–N(6)	76.67(18)	73.7(3)
N(4)–Fe(1)–N(1)	82.54(19)	107.56(10)
N(3)–Fe(1)–N(1)	78.59(18)	75.1(3)
N(6)–Fe(1)–N(1)	154.89(19)	102.29(14)
N(4)–Fe(1)–O(3)	173.04(17)	—

angle being 172.3(3)° (Table 1), whereas the imidazole nitrogens (N1, N4 and N6) of the supporting ligand constitute the equatorial plane. The phenolic oxygen O1 and the carboxylate oxygen O3 forms intramolecular hydrogen bond, whereas the phenolic oxygen O3 forms intermolecular hydrogen bond with a perchlorate oxygen. The perchlorate anions are in hydrogen bonding interaction with one non-coordinated nitrogen of the benzimidazole ring of the supporting ligand of another molecule. Additionally, the carboxylate oxygen O3 of one molecule forms hydrogen bond with a nitrogen of imidazole ring of another molecule. All these hydrogen bonding interactions give rise to a one-dimensional architecture in the lattice structure of **3a**. Although the carboxylate group of DHN-H binds in monodentate mode in **3a**, the ligand is known to form both five and six-coordinate iron complexes.<sup>23</sup> Although the structure of **3a** is found to be five-coordinate, the bulk solid may contain six-coordinate iron(II) complex with asymmetric bidentate binding of the carboxylate group of DHN-H. In fact, the FT-IR spectra of the complexes show sharp bands in the regions 1575–1590 cm<sup>-1</sup> and 1435–1440 cm<sup>-1</sup> attributable to  $\nu_a(\text{COO})$  and  $\nu_s(\text{COO})$ , respectively. The energy difference  $\Delta\nu(\text{COO})$  of <200 cm<sup>-1</sup> is consistent with the bidentate binding mode of the carboxylate groups in all the iron(II) complexes.<sup>24</sup> The iron(II) complexes are expected to retain their geometries in solution. However, the IR spectra of the complexes in solution could not be measured due to their sensitivity toward oxygen.

### Reactivity of iron complexes toward dioxygen

All the iron(II) complexes exhibit charge transfer (CT) bands below 400 nm. The high energy bands likely arise from ligand-based transitions.<sup>18</sup> Although the complexes are stable under

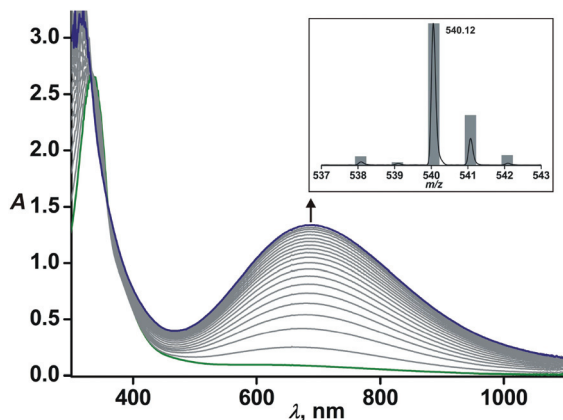


Fig. 2 UV-vis spectral changes of **1** (1 mM in CH<sub>3</sub>CN) upon exposure to dioxygen at 298 K. Inset: ESI-mass spectrum (positive ion mode in CH<sub>3</sub>CN) of the solution after 1 h of reaction.

inert atmosphere both in the solid state, they react rapidly with dioxygen in solution. Exposure of an acetonitrile solution of **1** to dioxygen results in a blue violet solution exhibiting a broad CT band at 690 nm (Fig. 2). The ESI-mass spectrum of the solution shows an ion peak at  $m/z$  540.12 with the isotope distribution pattern calculated for  $[(6\text{-Me}_3\text{-TPA})\text{Fe}(\text{GN})]^+$  (Fig. 2, inset). Similarly, **2** and **3** when allowed to react separately with O<sub>2</sub>, CT bands are formed at 700 nm and 620 nm, respectively (Fig. S9<sup>†</sup>). Each of the oxidized solutions of **1**, **2** and **3** exhibits rhombic signal at  $g = 4.2$  in the X-band EPR spectrum at 77 K indicating the formation of the corresponding iron(III)-gentsiate complexes. It has been reported that the iron(III)-catecholate/aminophenolate complexes of N4 ligands display bands in the visible region due to the CT transitions from catecholate/aminophenolate to iron(III).<sup>25–33</sup> The iron(III)-salicylate complexes,  $[(\text{BPMEN})\text{Fe}^{\text{III}}(\text{salicylate})]^+$  and  $[\text{Fe}^{\text{III}}(\text{TPA})(5\text{-Cl-salicylate})]^+$ , have been reported to display phenolate to iron(III) CT bands at 590 nm and 560 nm, respectively.<sup>34,35</sup> The bands in the visible region for the oxidized complexes, therefore, could be attributed to the GN-to-iron(III) CT transitions. Thus phenolate (of GN) is coordinated to the metal centre in each of the iron(III) species. The other site of the six-coordinate iron(III) complex must be occupied by one of the carboxylate oxygens *via* reorganization from bidentate to monodentate coordination. The crystal structures of both  $[(\text{BPMEN})\text{Fe}^{\text{III}}(\text{salicylate})]^+$  and  $[\text{Fe}^{\text{III}}(\text{TPA})(5\text{-Cl-salicylate})]^+$  revealed bidentate coordination of salicylate through one carboxylate oxygen and the phenolate oxygen.<sup>34,35</sup> By analogy with the reported iron(III)-salicylate complexes, a similar bidentate binding of gentsiate is expected in each of the oxidized complexes from **1**, **2** and **3**. The iron(III)-gentsiate complexes are stable and do not undergo further reaction with dioxygen. Gentsiate was quantitatively recovered from the final reaction solution of **3** (Fig. S10<sup>†</sup>).

Since DHN-H<sub>2</sub> is an active substrate of GDO, the iron(II)-DHN-H complexes (**1a**, **2a**, and **3a**) were investigated to evaluate the effect of supporting ligand on the oxidative transform-

ation of co-ligand. Complex **1a** reacts with dioxygen over a period of 20 min, during which time the solution turned deep green with the formation of broad CT bands at 700 nm and 840 nm (Fig. 3a). Similar spectral changes are observed with **2a** and **3a** (Fig. S11 and S12<sup>†</sup>). In iron(III)-phenolate complexes, phenolate-to-iron(III) CT transitions originate from the  $p\pi$  to the  $d\sigma^*$  and  $d\pi^*$  orbitals of Fe(III). The positions of these bands are dependent on the Lewis acidity of iron center, which is tuned by supporting ligand.<sup>25</sup> The weak donor 6-Me<sub>3</sub>-TPA ligand stabilises the  $d\pi^*$  orbital leading to a decrease in  $d\pi^*$ -phenolate orbital energy gap and therefore the LMCT band is shifted to lower energy. Therefore a large difference in the two bands is observed in the case of **1a**. For other two complexes (**2a** and **3a**) of relatively strong donor ligands, the low energy bands are less shifted and appear as broad peaks. The basic benzimidazole groups in TbimA destabilise the  $d$ -orbital leading to higher LMCT energy for the oxidised species of **3a**. Additionally, the nature of co-ligand also affects the CT energy. The iron(III)-5-methoxysalicylate species of the BPMEN ligand, generated from the precursor iron(II) complex upon oxidation by O<sub>2</sub>, shows the CT band at 650 nm, whereas the same is observed at lower energy (680 nm) for the BPMEN-iron(III)-1-

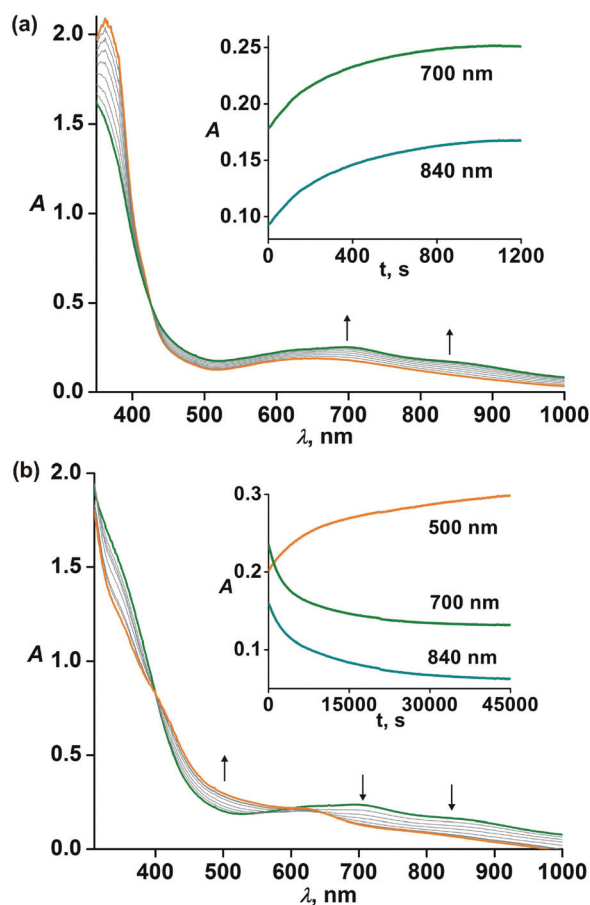


Fig. 3 Optical spectral changes of complex **1a** (0.5 mM in acetonitrile) in the reaction with dioxygen at 298 K. (a) Reaction in the first 20 min and (b) reaction in the next 12 h. Inset: Plot of absorbance vs. time.

hydroxy-2-naphthoate species (*vide infra*). Introduction of an additional *p*-OH group on salicylate or naphthoate ring further shifts the CT band to lower energy as observed in the iron(III)-gentisate or iron(III)-DHN species (Fig. 3a, S9a and S11a†).

In the second step of the reactions, the CT bands decay with time indicating the oxidation of DHN. For **1a**, the 700 nm and 840 nm bands decay concomitant with the formation of a band at 460 nm band within a period of around 12 h (Fig. 3b). For complex **2a**, the intensity of the band at around 760 nm diminishes in 2 h (Fig. S11†). Similar behaviour is observed for complex **3a** (Fig. S12†). The time-dependent X-band EPR data collected at 77 K during the reaction of **2a** with O<sub>2</sub> reveal that the rhombic signal at *g* = 4.2 attains maximum intensity after 2 min and then gradually decreases (Fig. S13†). The EPR data are consistent with the formation of a transient iron(III)-DHN species as observed in the time-dependent optical spectra. The ESI-mass spectrum of the final oxidized solution of **1a** exhibits an ion peak at *m/z* 760.26 calculated for [(6-Me<sub>3</sub>-TPA)Fe(BNTHC) + H]<sup>+</sup> (BNTHC = [2,2'-binaphthalene]-1,1',4,4'-tetrone-3-hydroxy-3'-carboxylic acid) (Fig. S14a†). However, the product formed from **2a** is different as observed from the ESI-mass spectrum of the oxidized solution. In this case, the ion peak at *m/z* 727.54 is assigned to [(BPMEN)Fe(BNTD) + H]<sup>+</sup> (BNTD = [2,2'-binaphthalene]-1,1',4,4'-tetrone, 3,3'-dicarboxylic acid) (Fig. S14b†).

The organic products from the oxidized solutions of **1a** and **2a**, after removal of the metal ion by acid workup, were separately isolated and analyzed by <sup>1</sup>H NMR spectroscopy. The spectral analyses clearly suggest that 1,4-dihydroxy-2-naphthoic acid does not yield any C–C bond cleavage products, rather undergoes oxidative C–C coupling reaction to form [2,2'-binaphthalene]-1,1',4,4'-tetrone,3-hydroxy-3'-carboxylic acid (BNTHC) from **1a** and [2,2'-binaphthalene]-1,1',4,4'-tetrone, 3,3'-dicarboxylic acid (BNTD) from **2a** (Fig. 4 and Scheme 3). Of note, both the coupled products display similar spectral patterns in NMR spectroscopy but the spectrum for BNTHC (Fig. 4a) is not as well resolved as BNTD (Fig. 4b) due to the absence of symmetry in the former. The peaks at δ 8.35–8.05 (m, 4H), 7.95–7.60 (m, 4H) and 13.76 (b) ppm in the <sup>1</sup>H NMR spectrum are assigned to the phenyl rings of the coupled product. Around 40% and 42% coupled product is estimated from **1a** and **2a**, respectively, by <sup>1</sup>H NMR quantification using 1,3,5-trimethoxybenzene as an internal standard. The iron(II)-DHN complex (**3a**), in the reaction with dioxygen, affords the same organic product (Table 2).

To confirm the structure and composition of the oxidized complexes, X-ray quality single crystals were grown. The structures established the oxidative coupling of two DHN moieties resulting in the formation of [(6-Me<sub>3</sub>-TPA)Fe<sup>II</sup>(BNTHC)] (**1<sup>Ox</sup>**) and [(BPMEN)Fe<sup>II</sup>(BNTD)] (**2<sup>Ox</sup>**) from **1a** and **2a**, respectively (Experimental section). The iron centre in each of the complex is ligated by four nitrogen donors from the supporting ligand (6-Me<sub>3</sub>-TPA or BPMEN) and two oxygen donors from BNTHC (for **1<sup>Ox</sup>**) or from BNTD (**2<sup>Ox</sup>**) (Fig. 5). In **1<sup>Ox</sup>**, the axial positions of the distorted octahedron are occupied by the one pyridine nitrogen N2 and one oxygen atom O1 with the O1–Fe–N2

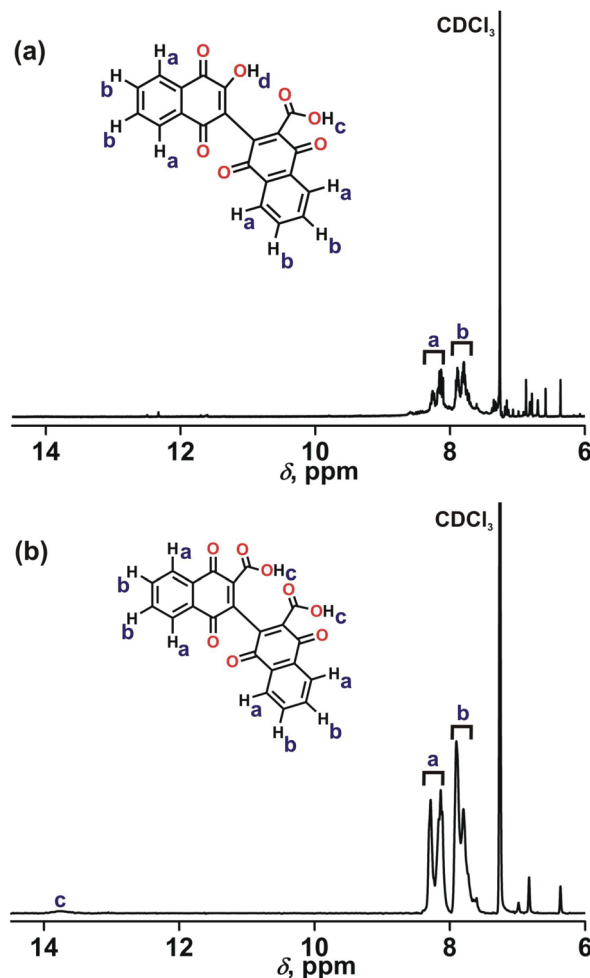
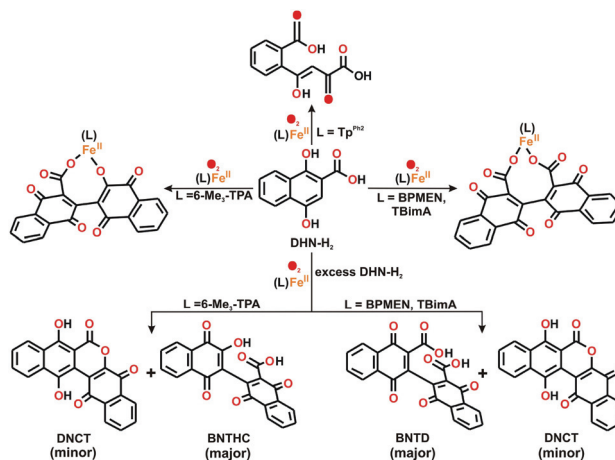


Fig. 4 <sup>1</sup>H NMR spectrum (300 MHz, CDCl<sub>3</sub> at 298 K) of the organic product from the oxidized solution of (a) **1a** and (b) **2a**.



Scheme 3 Oxidative transformation of DHN on the iron(II) complexes.

angle of 172.02(15)° (Table 3). The Fe–N bond distance lies within 2.211–2.240 Å, which are typical of high-spin iron(II) complex. The BNTHC binds in a bidentate fashion through

**Table 2** Products formed in the reactions of iron(II)–GN–H/DHN–H complexes with dioxygen

Iron(II) complex	Product derived from iron(II) complex (CT band, nm)	Organic product	Yield (%)
[(6-Me <sub>3</sub> -TPA)Fe <sup>II</sup> (GN-H)] <sup>+</sup> (1)	[(6-Me <sub>3</sub> -TPA)Fe <sup>III</sup> (GN)] <sup>+</sup> (690)	—	—
[(BPMEN)Fe <sup>II</sup> (GN-H)] <sup>+</sup> (2)	[(BPMEN)Fe <sup>III</sup> (GN)] <sup>+</sup> (700)	—	—
[(TBimA)Fe <sup>II</sup> (GN-H)] <sup>+</sup> (3)	[(TBimA)Fe <sup>III</sup> (GN)] <sup>+</sup> (620)	—	—
[(Tp <sup>Ph2</sup> )Fe <sup>II</sup> (GN-H)] <sup>a</sup>	—(640, 980) <sup>b</sup>	Un-identified C–C cleavage product	—
[(6-Me <sub>3</sub> -TPA)Fe <sup>II</sup> (DHN-H)] <sup>+</sup> (1a)	[(6-Me <sub>3</sub> -TPA)Fe <sup>II</sup> (BNTHC)](1 <sup>Ox</sup> )	BNTHC	40
[(BPMEN)Fe <sup>II</sup> (DHN-H)] <sup>+</sup> (2a)	[(BPMEN)Fe <sup>II</sup> (BNTD)](2 <sup>Ox</sup> )	BNTD	42
[(TBimA)Fe <sup>II</sup> (DHN-H)] <sup>+</sup> (3a)	[(TBimA)Fe <sup>II</sup> (BNTD)]	BNTD	38
[(Tp <sup>Ph2</sup> )Fe <sup>II</sup> (DHN-H)] <sup>a</sup>	—(720, 920) <sup>b</sup>	2'-Carboxy-4-hydroxybenzal-pyruvic acid	—

<sup>a</sup> Ref. 18. <sup>b</sup> CT band of the intermediate iron(III) species.

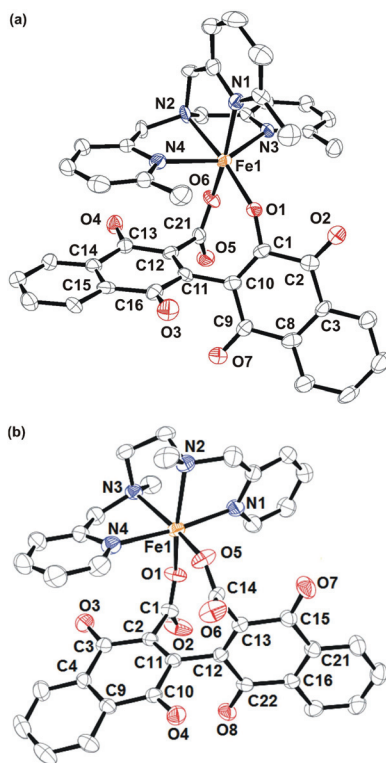


**Fig. 5** ORTEP plots of complexes (a) 1<sup>Ox</sup> and (b) 2<sup>Ox</sup> with 55% thermal ellipsoid parameters. All hydrogen atoms have been omitted for clarity.

**Table 3** Selected bond lengths (Å) and angles (°) for [(6-Me<sub>3</sub>-TPA)Fe<sup>II</sup>(BNTHC)] (1<sup>Ox</sup>)

Fe(1)–O(1)	1.983(3)	C(1)–O(1)	1.291(6)
Fe(1)–O(6)	2.114(4)	C(2)–O(2)	1.220(6)
Fe(1)–N(1)	2.240(4)	C(9)–O(7)	1.245(6)
Fe(1)–N(2)	2.211(4)	C(21)–O(6)	1.277(6)
Fe(1)–N(3)	2.281(4)	C(16)–O(3)	1.217(6)
Fe(1)–N(4)	2.295(4)	C(1)–C(10)	1.364(7)
C(10)–C(11)	1.488(7)	C(11)–C(12)	1.341(7)
C(3)–C(8)	1.404(8)	C(14)–C(15)	1.398(8)
O(6)–Fe(1)–N(1)	163.02(15)	O(1)–Fe(1)–N(2)	172.02(15)
N(3)–Fe(1)–N(4)	149.45(15)	O(1)–Fe(1)–O(6)	88.45(14)
O(6)–Fe(1)–N(2)	85.16(15)	O(1)–Fe(1)–N(1)	106.78(15)
N(2)–Fe(1)–N(1)	80.22(16)	O(1)–Fe(1)–N(3)	109.50(15)
O(6)–Fe(1)–N(3)	81.27(15)	N(2)–Fe(1)–N(3)	74.27(15)
N(1)–Fe(1)–N(3)	86.46(15)	O(1)–Fe(1)–N(4)	101.01(15)
O(6)–Fe(1)–N(4)	101.61(15)	N(2)–Fe(1)–N(4)	75.67(15)

one hydroxy oxygen and one carboxylate with the Fe1–O1 and Fe1–O6 distances of 1.983(3) and 2.114(4) Å, respectively. The complex displays an absorption band at 650 nm attributable to the iron(II)–BNTHC MLCT transition because of the presence of low-lying vacant  $\pi^*$  orbital of BNTHC. In the case of 2<sup>Ox</sup>, two pyridine nitrogens N1 and N4 occupy the axial positions with the N1–Fe1–N4 angle of 173.01(9)° (Table 4). The high-spin iron(II) center with the average Fe–N bond distance of 2.222(2) Å allows the BNTD to bind two carboxylate groups with the Fe1–O1 and Fe1–O5 distances of 2.048(2) and 2.050(2) Å, respectively. The bond parameters in both the complexes further confirm the presence of quinone moieties in BNTHC and BNTD. While the binding modes of BNTHC results in an eight-membered metallomacrocycle, BNTD forms a nine-membered ring comprising of one iron, two oxygens and six carbons. Therefore, the non-planar species, BNTHC and BNTD, may not be very stable in their non-coordinated forms.

Interestingly, when the reaction of 2a with dioxygen is carried out in the presence of excess (5 equiv.) DHN–H<sub>2</sub>, two compounds are isolated in a 3.5 : 1 ratio. While the BNTD is formed as a major product (with a TON of 2.1), a blue organic product, 8,13-dihydroxy-1*H*-benzo[*g*]naphtho[2,3-*c*]chromene-

**Table 4** Selected bond lengths (Å) and angles (°) for [(BPMEN)Fe<sup>II</sup>(BNTD)] (2<sup>Ox</sup>)

Fe(1)–O(1)	2.048(2)	Fe(1)–N(1)	2.186(2)
Fe(1)–O(5)	2.050(2)	Fe(1)–N(2)	2.255(2)
C(14)–O(5)	1.252(3)	Fe(1)–N(3)	2.252(2)
C(14)–O(6)	1.230(3)	Fe(1)–N(4)	2.195(3)
C(12)–C(13)	1.342(3)	C(1)–O(1)	1.244(3)
C(13)–C(14)	1.515(4)	C(1)–O(2)	1.222(3)
C(13)–C(15)	1.498(4)	C(1)–C(2)	1.526(3)
C(15)–O(7)	1.217(3)	C(2)–C(3)	1.484(4)
C(15)–C(16)	1.475(4)	C(3)–O(3)	1.214(3)
C(16)–C(21)	1.395(4)	C(3)–C(4)	1.491(4)
C(21)–C(22)	1.483(4)	C(4)–C(9)	1.394(4)
C(22)–O(8)	1.215(3)	C(9)–C(10)	1.473(4)
C(22)–C(12)	1.484(4)	C(10)–O(4)	1.221(3)
C(11)–C(12)	1.491(4)	C(10)–C(11)	1.489(3)
O(1)–Fe(1)–O(5)	104.97(9)	C(11)–C(2)	1.340(4)
O(1)–Fe(1)–N(1)	88.14(9)	N(1)–Fe(1)–N(3)	97.49(9)
O(5)–Fe(1)–N(1)	95.64(10)	N(4)–Fe(1)–N(3)	75.81(9)
O(1)–Fe(1)–N(4)	93.60(9)	O(1)–Fe(1)–N(2)	159.33(8)
O(5)–Fe(1)–N(4)	90.45(9)	O(5)–Fe(1)–N(2)	90.34(9)
N(1)–Fe(1)–N(4)	173.01(9)	N(1)–Fe(1)–N(2)	76.39(9)
O(1)–Fe(1)–N(3)	88.62(9)	N(4)–Fe(1)–N(2)	100.21(9)
O(5)–Fe(1)–N(3)	161.39(8)	N(3)–Fe(1)–N(2)	80.04(9)

5,7,14-trione (DNCT), isolated as a minor product (0.6 TON) (Experimental section). In the  $^1\text{H}$  NMR spectrum of DNCT, three sets of resonances are detected and the OH protons of naphthaquinol groups are found to be most downfield shifted. Two sets of aromatic protons appear in the region between 7.5 ppm and 8.5 ppm (Fig. 6). Different chemical environments of the aromatic protons of two terminal phenyl rings give rise to multiples peaks in that region.

The crystal structure of DNCT (**2F**) reveals that the molecule is planar containing a naphthaquinone lactone unit fused with a naphthaquinol unit (Fig. 7). While the C1–O2 and C8–O1 distance of 1.247(5) Å, 1.242(4) Å, respectively, are typical of a quinone group, the C13–O3 (1.306(4) Å) and C23–O4 (1.324(4) Å) distances indicate the presence of naphthaquinol group. Hydrogen bonding interactions between the keto and the hydroxyl group play vital roles in stabilising the planarity of naphthaquinol moiety (Fig. S15<sup>†</sup>). Complex **1a** also reacts with oxygen in the presence of excess DHN- $\text{H}_2$  to afford DNCT similar to that observed with **2a**.

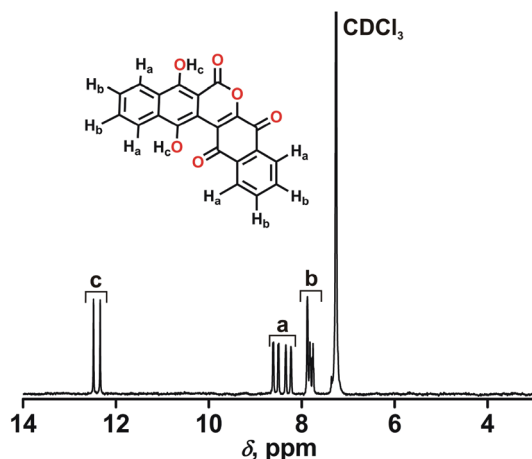


Fig. 6  $^1\text{H}$  NMR (500 MHz,  $\text{CDCl}_3$  at 298 K) spectrum of DNCT (**2F**) derived from the oxidized solution of **2a** in the presence of excess DHN- $\text{H}_2$ .

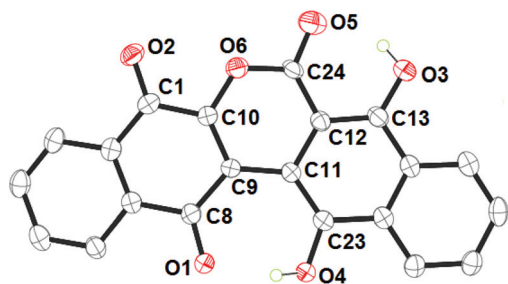
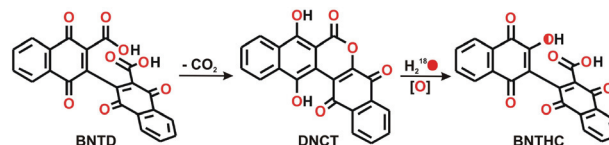


Fig. 7 ORTEP plot of **2F** with 45% ellipsoid probability. All hydrogen atoms except those on O3 and O4 have been omitted for clarity. Selected Bond distances (Å): C1–O2 1.247(5), C8–O1 1.242(4), C13–O3 1.306(4), C23–O4 1.324(4), C9–C10 1.392(5), C11–C12 1.443(5), C10–O6 1.370(4), C24–O(6) 1.362(5), C24–O5 1.254(5), C12–C24 1.422(5).

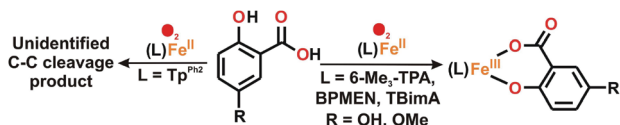
It is important to mention here that similar C–C coupling reactions take place in biological systems. Cytochrome P450, CYP158A2 isolated from *Streptomyces coelicolor*, has been reported to catalyse the C–C oxidative coupling of flavinols to biflavinol and triflavinol.<sup>36,37</sup> The flavinol polymer-based red-brown pigments are assumed to provide physical protection for the soil bacterium against the harmful effects of UV irradiation on genetic integrity.<sup>36,38</sup> Additionally, the planar compound DNCT (**2F**) and its open form analogue (BNTHC) bears similarity with the respective structure of WS-5995A and WS-5995C, the anticoccidial drugs possessing excellent protective activity against *Eimeria tenella* infection.<sup>39</sup> While WS-5995A/C have been synthesized using different protocols, low yields and/or multistep synthesis remained a major issue.<sup>40–42</sup> Thus, the unique single step transformation of DHN to BNTD/BNTHC and DNCT by the iron complex and  $\text{O}_2$  would provide a new synthetic protocol for the above compounds.

The structures of the oxidation products (**1<sup>Ox</sup>**, **2<sup>Ox</sup>** and **2F**) indicate that the three species (BNTD, DNCT and BNTHC) are related to each other (Scheme 4). In all the cases, BNTD is the C–C coupled product formed initially. The nonplanar BNTD is unlikely to bind to (6- $\text{Me}_3$ -TPA) $\text{Fe}^{\text{II}}$  unit to avoid steric interactions. Consequently, BNTD undergoes decarboxylation and lactonisation to afford DNCT. The more Lewis acidic iron centre with 6- $\text{Me}_3$ -TPA hydrolyses DNCT resulting in the formation of the iron(III)–BNTHC complex (**1<sup>Ox</sup>**). The intermediacy of DNCT in the conversion of BNTD to BNTHC was further established from a labelling experiment with  $\text{H}_2^{18}\text{O}$ . The ESI-mass spectrum of **1<sup>Ox</sup>** showing ion peak at  $m/z$  760.26 is shifted two mass unit higher at  $m/z$  762.27 (Fig. S16<sup>†</sup>). Thus, DNCT is converted to BNTHC upon hydrolysis with the incorporation of one oxygen atom from water. In the reaction, however, quinone moieties also exchange their oxygen atoms with water.<sup>43</sup> On the other hand, the sterically less demanding BPMEN ligand stabilises the iron(II)–BNTD complex (**2<sup>Ox</sup>**). In this case, DNCT is formed only in the presence of excess DHN- $\text{H}_2$ .

To understand the role of *para*-hydroxy group in the oxidative C–C coupling reaction, the reactivity of two related substrates (1-hydroxy-2-naphthoate and 5-methoxysalicylate) was investigated on the  $\text{Fe}^{\text{II}}$ (BPMEN) complex. In the reaction with dioxygen, **2b** and **2c** each forms the corresponding iron(III) complexes without any oxidation of the co-ligand (Scheme 5 and Fig. S17<sup>†</sup>). As observed earlier, these substrates were not oxidised by the ( $\text{Tp}^{\text{Ph}_2}$ ) $\text{Fe}^{\text{II}}$  complex and dioxygen.<sup>18</sup>



Scheme 4 Decarboxylation/lactonisation of the C–C coupled product of DHN- $\text{H}_2$  followed by hydrolysis.



**Scheme 5** Oxidative transformation of GN, HNA and 5-OMeSA on the iron(II) complexes.

From the experimental data discussed above and by comparing to those of the complex of the monoanionic facial N3 ligand ( $\text{Tp}^{\text{Ph}_2}$ ), it is obvious that geometry, denticity and stereoelectronic properties of the ligands control the reaction of 1,4-dihydroxy-2-naphthoic acid towards dioxygen. Additionally, it is not gentisate but the DHN forms the coupled product. Of note, neither the C–C bond cleavage product (2'-carboxy-4-hydroxybenzalpyruvic acid) nor C–C coupled product is observed in the control experiments with equimolar amounts of iron(II) salt and 1,4-dihydroxy-2-naphthoic acid with dioxygen (Experimental section).

Therefore, the iron(III)–DHN complex is an intermediate species initially formed in the reaction pathway leading to C–C coupled product. The same iron(III) species is formed from the iron(II) precursor upon treatment with  $\text{Ag}^+$  in the absence of oxygen (Experimental section and Fig. S18†). On the contrary, an iron(III)–DHN complex of the facial N3 ligand,  $\text{Tp}^{\text{Ph}_2}$ ,<sup>18</sup> has been reported to react with oxygen leading to C–C cleavage product. The yield of the coupled product remains less than 50% in all the complexes reported here supporting the fact that the second molecule of  $\text{DHN-H}_2$  is derived from another iron(II)–DHN–H complex. However, it is not clear if the reaction takes place in the coordination sphere all along the transformation. Further investigations are required to shed light on the mechanism of the dioxygen-dependent coupling reactions of DHN.

## Experimental

### Methods and equipment

All reagents were purchased from commercial sources and were used without further purification, unless otherwise mentioned. Solvents were distilled, dried and deoxygenated before use. Preparation and handling of air-sensitive iron(II) compounds were carried out under an inert atmosphere in a glove box. The ligands were synthesised following the procedure reported in the literature.<sup>21,44</sup> *Although no problem was encountered during the synthesis of the complexes, perchlorate salts are potentially explosive and should be handled with care!*<sup>45</sup>

Fourier transform infrared spectroscopy on KBr pellets was performed on a Shimadzu FT-IR 8400S instrument. Elemental analyses were performed on a PerkinElmer 2400 series II CHN analyzer. Electro-spray ionization (ESI) mass spectra were recorded with a Waters QTOF Micro YA263 instrument. Solution electronic spectra (single and time-dependent) were measured on an Agilent 8453 diode array spectrophotometer.

All room temperature NMR spectra were collected on a Bruker Avance 500 MHz spectrometer. Labelling experiments was carried out with  $\text{H}_2^{18}\text{O}$  (97 atom%) purchased from Sigma Aldrich.

### Synthesis of complexes

**[(6-Me<sub>3</sub>-TPA)Fe<sup>II</sup>(GN-H)](BPh<sub>4</sub>) (1).** To a solution (5 mL) of 6-Me<sub>3</sub>-TPA (0.33 g, 1 mmol) in methanol, a solution of iron(II) perchlorate hexahydrate (0.36 g, 1 mmol) in 5 mL methanol was added. Solid sodium gentisate powder was added to the solution and stirred for 4 h. A solution of sodium tetraphenylborate (0.26 g, 1 mmol) was added further to the mixture and stirred for 1 h. A light green solid was isolated by filtration from the mixture and dried. Single crystals suitable for X-ray diffraction were obtained by slow diffusion diethyl ether into a solution of the complex in a mixture of dichloromethane and methanol (1 : 1) Yield: 0.62 g (72%). Anal. Calcd for  $\text{C}_{52}\text{H}_{49}\text{BFeN}_4\text{O}_4$  (860.63 g mol<sup>-1</sup>): C, 72.57; H, 5.74; N, 6.51. Found: C, 72.29; H, 5.61; N, 6.63%. IR (KBr, cm<sup>-1</sup>): 3433(m), 3053(m), 2924(m), 2854(w), 1608(s), 1558(vs), 1541(vs), 1472(m), 1456(vs), 1394(m), 1337(m), 1244(w), 785(m), 735(s), 706(s), 611(m). ESI-MS (in positive ion mode,  $\text{CH}_3\text{CN}$ ):  $m/z$  333.12 (100%, [(6-Me<sub>3</sub>-TPA) + H]<sup>+</sup>), 541.15 (60%, [(6-Me<sub>3</sub>-TPA)Fe(GNH)]<sup>+</sup>). UV-vis in  $\text{CH}_3\text{CN}$ ;  $\lambda$ , nm ( $\epsilon$ , M<sup>-1</sup> cm<sup>-1</sup>): 332 (5400).  $\mu_{\text{eff}}$  (298 K): 4.8  $\mu_{\text{B}}$ . <sup>1</sup>H NMR in  $\text{CD}_3\text{CN}$  (500 MHz);  $\delta$  (ppm): 74.0 (6H, PyH $_{\beta}$ ), 51.3 (3H, PyH $_{\beta}$ ), 45.3 (3H, PyH $_{\gamma}$ ), 43.0 (3H, CH<sub>2</sub>Py), 26.9 (3H, CH<sub>2</sub>Py), 16.5 (1H, 1-OH), 14.1 (1H, 4-OH), 9.4 (1H, gentisate-3-H), 7.2(1H, gentisate-5-H), 7.0 (2H, gentisate-6-H), -49.5 (3H, PyH $_{\alpha}$ ).

**[(6-Me<sub>3</sub>-TPA)Fe<sup>II</sup>(DHN-H)](ClO<sub>4</sub>) (1a).** A methanolic solution (2 mL) of iron(II) perchlorate hexahydrate (0.18 g, 0.5 mmol) was added to a solution of 6-Me<sub>3</sub>-TPA (0.17 g, 0.5 mmol) in methanol (3 mL) and the resulting mixture was allowed to stir for 2 min. To the bright yellow solution, 1,4-dihydroxy-2-naphthoic acid (0.10 g, 0.5 mmol) and triethylamine (0.5 mmol, 70  $\mu\text{L}$ ) dissolved in 2 mL of methanol were added. The resulting green solution was then allowed to stir under nitrogen atmosphere for 6 h. The solution was dried under reduce pressure, filtered after addition of dichloromethane (5 mL) and the filtrate was concentrated to 1 mL. Diethyl ether (10 mL) was added to the concentrated reaction solution and the mixture was then stirred for another 2 h to obtain a green solid of the perchlorate salt of the complex 2. Yield: 0.26 g (75%). Anal. Calcd for  $\text{C}_{32}\text{H}_{31}\text{ClFeN}_4\text{O}_8 \cdot \text{CH}_2\text{Cl}_2$ : C, 51.09; H, 4.29; N, 7.22. Found C, 50.51; H, 4.82; N, 6.94. ESI-MS (positive ion mode in  $\text{CH}_3\text{CN}$ ):  $m/z$  (%) = 590.43 ( $\text{C}_{32}\text{H}_{31}\text{FeN}_4\text{O}_4$  expected at  $m/z$  = 590.16 for [(6-Me<sub>3</sub>-TPA)Fe<sup>II</sup>(DHN-H)]<sup>+</sup>). IR (KBr, cm<sup>-1</sup>): 3431(br), 3074(w), 2926(s), 2854(m), 2680(w), 1744(m), 1637(m), 1605(s), 1581(s), 1448(s), 1412(w), 1352(w), 1320(m), 1225(w), 1095(vs), 1012(w), 833(w), 779(s), 624(s), 560(w). UV-vis ( $\text{CH}_3\text{CN}$ );  $\lambda$ , nm ( $\epsilon$ , M<sup>-1</sup> cm<sup>-1</sup>): 365 (4100). <sup>1</sup>H NMR (400 MHz,  $\text{CD}_3\text{CN}$ , 298 K):  $\delta$  50.96, 44.73, 33.87, 15.63, 12.33, 9.27, 7.16, 5.44, 3.65, 3.41, 3.35, 3.19, 3.33, 1.80, 1.27, 1.12, 0.88, -23.29, -49.28 ppm.

**[(BPMEN)Fe<sup>II</sup>(GN-H)](ClO<sub>4</sub>) (2).** A methanolic solution (2 mL) of iron(II) perchlorate hexahydrate (0.18 g, 0.5 mmol)

was added to a solution of BPMEN (0.14 g, 0.5 mmol) in methanol (3 mL) and the resulting mixture was allowed to stir for 2 min. To the light yellow solution, gentisic acid and triethylamine (0.5 mmol, 70  $\mu$ L) dissolved in 2 mL of methanol were added. The resulting green solution was then allowed to stir under nitrogen atmosphere for 6 h. The solution was dried under reduce pressure, filtered after addition of dichloromethane (5 mL) and the filtrate was concentrated to 1 mL. Diethyl ether (10 mL) was added to the concentrated reaction solution and the mixture was then stirred for another 2 h to obtain a light green solid of the perchlorate salt of the complex **2**. Pure crystalline complex was obtained by recrystallization from a solvent mixture of dichloromethane and hexane (1:2). Yield: 0.20 g (68%). Anal. Calcd for  $C_{23}H_{27}ClFeN_4O_8$  (578.78 g mol<sup>-1</sup>): C, 47.73; H, 4.70; N, 9.68. Found C, 47.42; H, 4.55; N, 9.76. IR (KBr, cm<sup>-1</sup>): 3429(br), 3134(m), 3053(s), 2986(m), 2924(s), 2855(m), 1744(m), 1663(m), 1605(s), 1578(s), 1477(vs), 1447(vs), 1387(s), 1302(m), 1240(m), 1148(s), 1121(s), 1101(s), 1063(s), 1026(s), 812(m), 750(vs), 706(vs), 610(m), 467(m). UV-vis (CH<sub>3</sub>CN);  $\lambda$ , nm ( $\epsilon$ , M<sup>-1</sup> cm<sup>-1</sup>): 325 (3100). <sup>1</sup>H NMR (500 MHz, CD<sub>3</sub>CN, 298 K):  $\delta$  128.30, 109.28, 104.84, 101.80, 85.73, 75.91, 70.23, 51.63, 45.35, 42.38, 8.57, 7.82, 7.36, 4.43, -6.71 ppm.

**[(BPMEN)Fe<sup>II</sup>(DHN-H)](ClO<sub>4</sub>) (2a)**. Complex **2a** was synthesized according to the procedure described for complex **2** except that 1,4-dihydroxy-2-naphthoic acid (0.5 mmol) was added instead of gentisic acid. The complex was isolated in pure form by recrystallization from a solvent mixture of dichloromethane and hexane (1:2). Yield: 0.20 g (64%). Elemental analysis calcd (%) for  $C_{27}H_{29}ClFeN_4O_8$  (628.84 g mol<sup>-1</sup>): C 51.57, H 4.65, N 8.91; Found: C 51.28, H 5.01, N 8.87; IR (KBr): 3431(br), 3242(br), 3067(m), 29749 (m), 2932(m), 2677(s), 2490(m), 1661(m), 1587(vs), 1472(m), 1439 (vs), 1327(s), 1229(m), 1146(vs), 1090(vs), 1022(m), 976(m), 814(s), 768(vs), 629(vs), 592(m), 467(m) cm<sup>-1</sup>; ESI-MS (positive ion mode in CH<sub>3</sub>CN):  $m/z$  (%) 528.87 ( $C_{27}H_{29}FeN_4O_4$  expected at  $m/z$  529.15 for  $[(BPMEN)Fe^{II}(DHN-H)]^+$ ). UV-vis (CH<sub>3</sub>CN);  $\lambda$ , nm ( $\epsilon$ , M<sup>-1</sup> cm<sup>-1</sup>): 360 (6080). <sup>1</sup>H NMR (500 MHz, CD<sub>3</sub>CN, 298 K):  $\delta$  141.58, 118.34, 109.63, 79.94, 50.66, 43.58, 11.45, 8.27, 7.83, 7.36, 7.23, 6.54, 6.22, 4.36, 3.43 ppm.

**[(BPMEN)Fe<sup>II</sup>(HNA)](ClO<sub>4</sub>) (2b)**. Complex **2b** was synthesized according to the procedure described for complex **2a** except that 1-hydroxy-2-naphthoic acid (HNA-H) (0.09 g, 0.5 mmol) was used instead of DHN-H<sub>2</sub>. An off-white crystalline solid was isolated by recrystallization from a solvent mixture of dichloromethane and hexane (1:2). Yield: 0.20 g (65%). Anal. Calcd for  $C_{27}H_{29}ClFeN_4O_7$  (612.84 g mol<sup>-1</sup>): C, 52.92; H, 4.77; N, 9.14. Found C, 52.74; H, 5.03; N, 9.39. IR (KBr, cm<sup>-1</sup>): 3420(br), 3064(m), 2926(s), 2856(m), 2679(m), 1605(vs), 1585(vs), 1441 (vs), 1400(vs), 1302(m), 1144(vs), 1115(vs), 1090(vs), 1022(m), 978(m), 806(m), 773(m), 731(m), 662(m), 631(m), 581(m), 469(m), 378(m). <sup>1</sup>H NMR (500 MHz, CD<sub>3</sub>CN, 298 K):  $\delta$  107.75, 88.64, 60.51, 28.35, 15.91, 8.52, 8.24, 7.76, 7.35, 7.18, -5.92, -22.17 ppm. UV-Vis (CH<sub>3</sub>CN);  $\lambda$ , nm ( $\epsilon$ , M<sup>-1</sup> cm<sup>-1</sup>): 335 (4860).

**[(BPMEN)Fe<sup>II</sup>(5-OMeSA)](BPh<sub>4</sub>) (2c)**. Equimolar amounts of BPMEN (0.14 g, 0.5 mmol), iron(II) perchlorate hexahydrate

(0.18 g, 0.50 mmol), 5-methoxysalicylic acid (5-OMeSA-H; 0.08 g, 0.50 mmol), and triethylamine (70  $\mu$ L) in 5 mL of methanol were stirred under a nitrogen atmosphere for 6 h. The solution was concentrated to 1 mL, and diethyl ether (10 mL) was added. The mixture was then stirred for another 2 h to give a light green solid of the perchlorate salt of the complex  $[(BPMEN)Fe^{II}(5-OMeSA)](ClO_4)$ . A methanolic solution of sodium tetraphenylborate (0.17 g, 0.50 mmol) was added to the methanolic reaction solution to precipitate a light green solid. The solid was isolated by filtration, washed with methanol, and dried. Yield: 0.25 g (62%). Anal. Calcd for  $C_{48}H_{49}BF_4FeN_4O_4$  (812.58 g mol<sup>-1</sup>): C, 70.95; H, 6.08; N, 6.89. Found C, 70.70; H, 6.22; N, 6.73. IR (KBr, cm<sup>-1</sup>): 3483(br), 33138(m), 3053(s), 3001(m), 2926(m), 2858(m), 1734(m), 1632(m), 1605(s), 1576(vs), 1481(vs), 1441(s), 1377(m), 1302(m), 1263(m), 1126(m), 1030(m), 978(m), 816(m), 739(vs), 707(vs), 665(m), 613(m), 471(m), 366(m). <sup>1</sup>H NMR (500 MHz, CD<sub>3</sub>CN, 298 K):  $\delta$  140.06, 113.61, 80.13, 48.95, 41.83, 21.53, 12.63, 10.01, 7.29, 7.00, 6.85, 4.04 ppm. UV-vis (CH<sub>3</sub>CN);  $\lambda$ , nm ( $\epsilon$ , M<sup>-1</sup> cm<sup>-1</sup>): 325 (3940).

**[(TBimA)Fe<sup>II</sup>(GN-H)](GN) (3)**. To a stirring solution of the TBimA (0.20 g, 0.5 mmol) and iron(II) perchlorate hexahydrate (0.18 g, 0.5 mmol) in methanol (5 mL), a mixture of gentisic acid (0.15 g, 0.5 mmol) and triethylamine (70  $\mu$ L, 0.5 mmol) in methanol (5 mL) was added dropwise. The resulting solution was allowed to stir for 6 h to precipitate an off-white solid. The solid was filtered and washed several times with methanol. Yield: 0.16 g (42%). Anal. Calcd for  $C_{38}H_{31}FeN_7O_8$  (769.54 g mol<sup>-1</sup>): C, 59.31; H, 4.06; N, 12.74. Found C, 59.73; H, 4.05; N, 12.90. IR (KBr, cm<sup>-1</sup>): 3431(br), 3198(m), 3123(m), 3059(m), 2926(m), 2779(m), 1622(m), 1574(s), 1450(vs), 1385(s), 1340(m), 1277(m), 1240(m), 1144(s), 1117(vs), 1088(s), 1045(m), 1001(m), 962(m), 889(m), 835(m), 748(vs), 681(m), 631(vs), 559(m), 434(m). UV-vis (CH<sub>3</sub>CN);  $\lambda$ , nm ( $\epsilon$ , M<sup>-1</sup> cm<sup>-1</sup>): 330 (4330). <sup>1</sup>H NMR (500 MHz, CD<sub>3</sub>CN, 298 K):  $\delta$  67.25, 56.72, 40.32, 26.09, 16.18, 12.80, 7.51, 7.32, 6.72, 6.27, 4.49, 3.63 ppm.

**[(TBimA)Fe<sup>II</sup>(DHN-H)](ClO<sub>4</sub>) (3a)**. Complex **3a** was synthesized according to the procedure described for complex **2** except that 1,4-dihydroxy-2-naphthoic acid (0.5 mmol) was added instead of gentisic acid and TBimA was used in place of BPMEN. Single crystals of **3a** suitable for X-ray diffraction were isolated by recrystallization from a solvent mixture of dichloromethane and methanol (1:2). Yield: 0.26 g (69%). Anal. Calcd for  $C_{35}H_{28}ClFeN_7O_8$  (765.94 g mol<sup>-1</sup>): C, 54.88; H, 3.68; N, 12.80. Found C, 54.12; H, 3.84; N, 12.41. IR (KBr, cm<sup>-1</sup>): 3356 (br), 3063(m), 2924(m), 2853(m), 1624(m), 1587(s), 1452(vs), 1435(s), 1418(s), 1391(m), 1337(s), 1315(s), 1231(m), 1115(vs), 1092(vs), 1043(m), 1003(m), 849(m), 750(vs), 625(m), 594(m), 440(m). ESI-MS (positive ion mode, acetonitrile):  $m/z$  666.34 ( $C_{35}H_{28}FeN_7O_4$  expected at  $m/z$  666.49 for  $[(TBimA)Fe^{II}(DHN-H)]^+$ ), 408.31 ( $C_{24}H_{22}N_7$  expected at  $m/z$  408.48 for  $[(TBimA) + H]^+$ ). UV-vis in acetonitrile;  $\lambda$ , nm ( $\epsilon$ , M<sup>-1</sup> cm<sup>-1</sup>): 340 (5560). <sup>1</sup>H NMR (500 MHz, CD<sub>3</sub>CN, 295 K):  $\delta$  58.11, 41.02, 26.44, 17.20, 10.41, 9.77, 8.48, 7.97, 7.27, 6.50, 3.41 ppm.

**Analysis of organic products after the reaction of iron(II)-DHN complexes with dioxygen.** Each of the iron(II) complexes

(0.02 mmol) were separately dissolved in 10 mL of dioxygen-saturated dry acetonitrile and then the solution was allowed to stir at room temperature. After the reaction, the solvent was removed under vacuum and the residue was treated with 3 M hydrochloric acid solution (10 mL). The organic products were extracted with diethyl ether (3 × 15 mL) and the organic layer was dried over anhydrous sodium sulfate. After removal of solvent, the residue was analyzed by  $^1\text{H}$  NMR spectroscopy. Control experiments were performed with iron(II) perchlorate hexahydrate (0.02 mmol) and gentisic acid or 1,4-dihydroxy-2-naphthoic acid (0.02 mmol) following the same protocol as discussed above.

**[(6-Me<sub>3</sub>-TPA)Fe<sup>II</sup>(BNTCH)] (1<sup>Ox</sup>).** The iron(II) complex **1a** (0.03 g, 0.04 mmol) was dissolved in dry acetonitrile (2 mL) and pure oxygen gas was bubbled through the solution. The oxygenated solution was stirred at room temperature under oxygen atmosphere for 12 h. The solution was then concentrated and the slow evaporation of the solution gives X-ray quality single crystal within a week. ESI-MS (positive ion mode in CH<sub>3</sub>CN):  $m/z$  760.26 (C<sub>42</sub>H<sub>33</sub>FeN<sub>4</sub>O<sub>7</sub> expected at  $m/z$  760.17 for {[(6-Me<sub>3</sub>-TPA)Fe<sup>II</sup>(BNTCH)] + H<sup>+</sup>}). UV-vis (CH<sub>3</sub>CN);  $\lambda$ , nm ( $\epsilon$ , M<sup>-1</sup> cm<sup>-1</sup>): 650 (500).  $^1\text{H}$  NMR (500 MHz, CD<sub>3</sub>CN, 298 K):  $\delta$  48.41, 37.18, 17.15, 9.87, 7.24, 5.43, 3.63, 3.41, 2.59, 1.12, 1.09, -20.44, -24.71 ppm.

**Isolation of [(BPMEN)Fe<sup>II</sup>(BNTD)] (2<sup>Ox</sup>).** The iron(II) complex **2a** (0.03 g, 0.05 mmol) was dissolved in dry acetonitrile (2 mL) and pure oxygen gas was bubbled through the solution. The oxygenated solution was stirred at room temperature under oxygen atmosphere for 4 h. The solvent was then evaporated and the residue was dissolved in dichloromethane (1 mL). Pure crystalline complex was obtained by recrystallization from a solvent mixture of dichloromethane and diethyl ether (1 : 1). Yield: 0.014 g (42%). Anal. Calcd for C<sub>38</sub>H<sub>30</sub>FeN<sub>4</sub>O<sub>8</sub> (726.51 g mol<sup>-1</sup>): C, 62.82; H, 4.16; N, 7.71. Found C, 63.23; H, 4.22; N, 7.78. IR (KBr, cm<sup>-1</sup>): 3427(br), 2922(s), 2854(m), 1625(br), 1448(m), 1284(w), 1115(vs), 1091(s), 787(m), 457(s), 424(s). ESI-MS (positive ion mode in CH<sub>3</sub>CN):  $m/z$  727.54 (C<sub>38</sub>H<sub>31</sub>FeN<sub>4</sub>O<sub>8</sub> expected at  $m/z$  727.54 for {[(BPMEN)Fe<sup>II</sup>(BNTD)] + H<sup>+</sup>}). UV-vis (CH<sub>3</sub>CN);  $\lambda$ , nm ( $\epsilon$ , M<sup>-1</sup> cm<sup>-1</sup>): 370 (sh).  $^1\text{H}$  NMR (500 MHz, CD<sub>3</sub>CN, 298 K):  $\delta$  85.05, 73.45, 54.39, 47.46, 23.23, 17.15, 8.85, 7.87, 7.34, 3.39, 2.26, 1.17 ppm.

**Isolation of DNCT (2F).** The iron(II) complex **2a** (0.03 g, 0.05 mmol) was dissolved in dry acetonitrile along with excess DHN-H<sub>2</sub> (0.05 g, 0.25 mmol). Pure oxygen gas was bubbled through the solution, and the mixture was stirred at room temperature under oxygen atmosphere for 12 h. Blue single crystals suitable for X-ray diffraction were obtained by slow evaporation of the solvent of the reaction solution. Yield: 0.01 g (60%). Anal. Calcd for C<sub>21</sub>H<sub>10</sub>O<sub>6</sub> (358.3 g mol<sup>-1</sup>): C, 70.39; H, 2.81. Found C, 69.34; H, 2.18. IR (KBr, cm<sup>-1</sup>): 3446 (br), 2923(vs), 2854(m), 1683(s), 1547(m), 1458(m), 1394(m), 1344(m), 1298(m), 1238 (w), 1153(w), 1090(m), 779(w), 673(w). ESI-MS (positive ion mode in CH<sub>3</sub>CN):  $m/z$  359.38 (C<sub>21</sub>H<sub>11</sub>O<sub>6</sub> expected at  $m/z$  359.3 for [DNCT + H<sup>+</sup>]). UV-vis (CH<sub>3</sub>CN);  $\lambda$ , nm ( $\epsilon$ , M<sup>-1</sup> cm<sup>-1</sup>): 590 (750).  $^1\text{H}$  NMR (500 MHz, CD<sub>3</sub>CN, 298 K):  $\delta$  12.42 (s), 12.34(s), 8.62–8.61(d), 8.51–8.49(d), 8.34(s), 8.23(s), 7.88–7.74(m) ppm.

**Analyses of BNTD and DNCT isolated from the reaction between 2a and dioxygen in the presence of excess DHN-H<sub>2</sub>.** The complex **2a** (0.02 mmol) was dissolved in 10 mL of dioxygen-saturated dry acetonitrile along with DHN-H<sub>2</sub> (5 equiv.). The solution was then allowed to stir at room temperature for overnight. After the reaction, the solvent was removed under vacuum and the residue was treated with 3 M HCl solution (10 mL). BNTD was isolated through extraction with diethyl ether (3 × 15 mL) and the organic layer was dried over anhydrous sodium sulfate. Removal of the solvent afforded BNTD. Further extraction of the aqueous phase with dichloromethane (3 × 15 mL) resulted in the isolation of DNCT. Both the compounds were separately analyzed and quantified by  $^1\text{H}$  NMR spectroscopy using 1,3,5-trimethoxybenzene as an internal standard.

**Reaction of the iron(II) complex with TEMPO radical or Ag<sup>+</sup> in the absence of dioxygen.** Complex **2a** (1 mM) was dissolved in oxygen-free dry acetonitrile in a cuvette. Silver sulphate (1 equiv.) was dissolved in dry acetonitrile in a vial. When the solution of Ag<sup>+</sup> was added to the solution of the complex under nitrogen atmosphere, a green species was formed. The optical spectrum of the green species bears resemblance to the species formed in the reaction between **2a** and dioxygen. The green species formed in this condition was stable for hours under inert atmosphere but undergoes further reaction upon exposure to dioxygen.

**X-ray crystallographic data collection, refinement and solution of the structure.** Single crystal X-ray data of the complexes were collected at 100 K using Mo K $\alpha$  ( $\lambda$  = 0.7107 Å) radiation on a SMART APEX diffractometer equipped with CCD area detector. Data collection, data reduction, structure solution/refinement were carried out using the software package of APEX II.<sup>46</sup> All structures were solved by direct method and subsequent Fourier analyses and refined by the full-matrix least-squares method based on  $F^2$  with all observed reflection.<sup>47</sup> The non-hydrogen atoms were treated anisotropically. The hydrogen atoms were geometrically fixed. SQUEEZE was applied to intensities data of **3a** and **2<sup>Ox</sup>** to take into account the disordered solvent molecules.<sup>48</sup> CCDC 1832200, 1832201, 1940079, 1832208 and 1832238 contain the supplementary crystallographic data for **1**, **3a**, **1<sup>Ox</sup>**, **2<sup>Ox</sup>** and **2F**, respectively.†

## Conclusions

We have isolated and characterised a series of iron(II)-gentisate/1,4-dihydroxy-2-naphthoate complexes of nitrogen rich ligands to investigate the role of supporting ligand in tuning the dioxygen reactivity and subsequent transformation of metal-coordinated co-ligands. The solid-state structures of the complexes indicate that gentisate/1,4-dihydroxy-2-naphthoate anion binds to the iron(II) center either in a monodentate or bidentate mode through their carboxylate group, but not through the phenolic OH groups. The iron(II)-1,4-dihydroxy-2-naphthoate complexes of N4 ligand react with molecular oxygen to undergo oxidation of the 1,4-dihydroxy-2-naphthoate

resulting in the formation of C–C coupled products whereas the iron(II)–gentsiate complexes form the corresponding iron(III)–gentsiate species. These results demonstrate the importance of the naphthoate moiety in the oxidative C–C coupling reaction. The presence of *para*-hydroxy group on the 1,4-dihydroxy-2-naphthoate substrate is essential for this unique oxidative C–C coupling reaction. This work highlights the influence of supporting ligands and of the co-ligand in directing the reactivity of model iron(II)–gentsiate/1,4-dihydroxy-2-naphthoate complexes, and thus supports the natural selection of the ‘facial N<sub>3</sub> motif’ at the active site of the gentsiate-1,2-dioxygenase.

## Conflicts of interest

There are no conflicts to declare.

## Acknowledgements

TKP gratefully acknowledges the Science and Engineering Research Board (SERB), India for the financial support (Project: EMR/2014/000972). RR, SM and SB thank the Council of Scientific and Industrial Research (CSIR), India for research fellowships.

## Notes and references

- S. Fetzner, *Appl. Environ. Microbiol.*, 2012, **78**, 2505–2514.
- F. H. Vaillancourt, J. T. Bolin and L. D. Eltis, *Crit. Rev. Biochem. Mol. Biol.*, 2006, **41**, 241–267.
- M. R. Harpel and J. D. Lipscomb, *J. Biol. Chem.*, 1990, **265**, 22187–22196.
- T.-C. Feng, C.-Z. Cui, F. Dong, Y.-Y. Feng, Y.-D. Liu and X.-M. Yang, *J. Appl. Microbiol.*, 2012, **113**, 779–789.
- M. R. Harpel and J. D. Lipscomb, *J. Biol. Chem.*, 1990, **265**, 6301–6311.
- J. Werwath, H. Arfamm, D. H. Pieper, K. N. Timmis and R. Wittich, *J. Bacteriol.*, 1998, **180**, 4171–4176.
- Y. Feng, H. E. Khoo and C. L. Poh, *Appl. Environ. Microbiol.*, 1999, **65**, 946–950.
- S. Luo, D. Q. Liu, H. Liu and N. Y. Zhou, *Microbiol. Res.*, 2006, **161**, 138–144.
- D. J. Fairley, G. Wang, C. Rensing, I. L. Pepper and M. J. Larkin, *Appl. Microbiol. Biotechnol.*, 2006, **73**, 691–695.
- L. Huang, H. Hu, H. Tang, Y. Liu, P. Xu, J. Shi, K. Lin, Q. Luo and C. Cui, *Sci. Rep.*, 2015, **5**, 14307.
- D. J. Hopper, P. J. Chapman and S. Dagley, *Biochem. J.*, 1968, **110**, 798–800.
- R. C. Bayly, P. J. Chapman, S. Dagley and D. Di Berardino, *J. Bacteriol.*, 1980, **143**, 70–77.
- J.-P. Hintner, C. Lechner, U. Riegert, A. E. Kuhm, T. Storm, T. Reemtsma and A. Stolz, *J. Bacteriol.*, 2001, **183**, 6936–6942.
- M. Ferraroni, I. Matera, S. Bürger, S. Reichert, L. Steimer, A. Scozzafava, A. Stolz and F. Briganti, *FEBS J.*, 2013, **280**, 1643–1652.
- J. Chen, W. Li, M. Wang, G. Zhu, D. Liu, F. Sun, N. Hao, X. Li, Z. Rao and X. C. Zhang, *Protein Sci.*, 2008, **17**, 1362–1373.
- S.-I. Hirano, M. Morikawa, K. Takano, T. Imanaka and S. Kanaya, *Biosci. Biotechnol. Biochem.*, 2007, **71**, 192–199.
- M. A. Adams, V. K. Singh, B. O. Keller and Z. Jia, *Mol. Microbiol.*, 2006, **61**, 1469–1484.
- R. Rahaman, B. Chakraborty and T. K. Paine, *Angew. Chem., Int. Ed.*, 2016, **55**, 13838–13842.
- Y. Zang, T. E. Elgren, Y. Dong and L. Que Jr., *J. Am. Chem. Soc.*, 1993, **115**, 811–813.
- A. W. Addison, T. N. Rao, J. Reedijk, J. van Rijn and G. C. Verschoor, *J. Chem. Soc., Dalton Trans.*, 1984, 1349–1356.
- B. Chakraborty, R. D. Jana, R. Singh, S. Paria and T. K. Paine, *Inorg. Chem.*, 2017, **56**, 359–371.
- C.-C. Tsou, W.-L. Yang and W.-F. Liaw, *J. Am. Chem. Soc.*, 2013, **135**, 18758–18761.
- R. M. Buchanan, R. J. O'Brien, J. F. Richardson and J.-M. Latour, *Inorg. Chim. Acta*, 1993, **214**, 33–40.
- K. Nakamoto, *Infrared and Raman Spectra of Inorganic and Coordination Compounds*, John Wiley, New York, 4th edn, 1986.
- H. G. Jang, D. D. Cox and L. Que Jr., *J. Am. Chem. Soc.*, 1991, **113**, 9200–9204.
- Y.-M. Chiou and L. Que Jr., *Inorg. Chem.*, 1995, **34**, 3577–3578.
- D.-H. Jo, Y.-M. Chiou and L. Que Jr., *Inorg. Chem.*, 2001, **40**, 3181–3190.
- H. Chun, E. Bill, E. Bothe, T. Weyhermüller and K. Wieghardt, *Inorg. Chem.*, 2002, **41**, 5091–5099.
- K. S. Min, T. Weyhermüller and K. Wieghardt, *Dalton Trans.*, 2003, 1126–1132.
- P. Halder, S. Paria and T. K. Paine, *Chem. – Eur. J.*, 2012, **18**, 11778–11787.
- B. Chakraborty and T. K. Paine, *Angew. Chem., Int. Ed.*, 2013, **52**, 920–924.
- B. Chakraborty, S. Bhunya, A. Paul and T. K. Paine, *Inorg. Chem.*, 2014, **53**, 4899–4912.
- S. Chatterjee and T. K. Paine, *Inorg. Chem.*, 2015, **54**, 1720–1727.
- S. Taktak, M. Flook, B. M. Foxman, L. Que Jr. and E. V. Rybak-Akimova, *Chem. Commun.*, 2005, 5301–5303.
- N. Y. Oh, M. S. Seo, M. H. Lim, M. B. Consugar, M. J. Park, J.-U. Rohde, J. Han, K. M. Kim, J. Kim, L. Que Jr. and W. Nam, *Chem. Commun.*, 2005, 5644–5646.
- B. Zhao, F. P. Guengerich, A. Bellamine, D. C. Lamb, M. Izumikawa, L. Lei, L. M. Podust, M. Sundaramoorthy, J. A. Kalaitzis, L. M. Reddy, S. L. Kelly, B. S. Moore, D. Stec, M. Voehler, J. R. Falck, T. Shimada and M. R. Waterman, *J. Biol. Chem.*, 2005, **280**, 11599–11607.
- B. Zhao, D. C. Lamb, L. Lei, S. L. Kelly, H. Yuan, D. L. Hachey and M. R. Waterman, *Biochemistry*, 2007, **46**, 8725–8733.

- 38 N. Funa, M. Funabashi, Y. Ohnishi and S. Horinouchi, *J. Bacteriol.*, 2005, **187**, 8149–8155.
- 39 H. Ikushima, M. Okamoto, H. Tanaka, O. Ohe, M. Kohsaka, H. Aoki and H. Imanaka, *J. Antibiot.*, 1980, **33**, 1107–1113.
- 40 M. Watanabe, M. Date and S. Furukawa, *Chem. Pharm. Bull.*, 1989, **37**, 292–297.
- 41 G. Qabaja and G. B. Jones, *J. Org. Chem.*, 2000, **65**, 7187–7194.
- 42 G. Qabaja, E. M. Perchellet, J.-P. Perchellet and G. B. Jones, *Tetrahedron Lett.*, 2000, **41**, 3007–3010.
- 43 A. Karich, M. Kluge, R. Ullrich and M. Hofrichter, *AMB Express*, 2013, **3**, 5.
- 44 G. J. P. Britovsek, J. England and A. J. P. White, *Inorg. Chem.*, 2005, **44**, 8125–8134.
- 45 W. C. Wolsey, *J. Chem. Educ.*, 1973, **50**, A335–A337.
- 46 *APEX 2, v2.1-0 ed*, Bruker AXS, Madison, WI, 2006.
- 47 G. M. Sheldrick, *SHELXL-97, Program for crystal structure refinement*, University of Göttingen, Göttingen, Germany, 1997.
- 48 P. van der Sluis and A. L. Spek, *Acta Crystallogr., Sect. A: Found. Crystallogr.*, 1990, **46**, 194–201.